SUPPLEMENTAL METHODS

Cell differentiation, Virues and Infections: The human myelomonocytic cell line KG-1[14] was differentiated into iDC as indicated in Supplemental Table 1. The monocytic cell line THP-1 was differentiated into macrophages with PMA (200 nM).[15] Human PBMCs were obtained from the Boston Children's Hospital blood bank. CD14+ monocytes were differentiated into iDC with GM-CSF (100 ng/ml) and IL-4 (50 ng/ml) or into MDM with M-CSF (100 ng/ml). Experiments were carried out with either the dual tropic HIV_{SF2} or the CCR5 tropic HIV_{Bal}. iDC and macrophages were infected with HIV_{SF2}-Flag Tat (20 ng of p24 per $1x10^6$ cells) for 6 hours and then resuspended with fresh medium and maintained in culture for 7-10 days. For the inhibition experiments, macrophages were infected as above with HIV_{Bal} and after 6 hours resuspended with fresh medium in the presence or absence of inhibitors of p38 (SB203580 and PH797804) and JNK (AS601245). Seven days post infection, cells were collected for RNA isolation and the supernatants were used for functional assay. HIv infetivity on day 10 ranged between 40 and 50%, when cells were stained with an anti-Flag antibody.

Chromatin immunoprecipitation (ChIP) and DNA microarray analysis (ChIP-Chip): For ChIP cells were infected with adenoviruses, subsequently cells were lysed and cell lysates were cross-linked and sonicated to yield an average DNA fragment of 500 bps. The sheared chromatin was incubated with protein G magnetic beads (Invitrogen) coupled to anti-FLAG (Sigma M2) monoclonal antibodies (Santa Cruz Biotechnology). This antibody was used because of its lack of background in ChIP experiments.[8,18,] Amplified DNA was labeled and purified using Bioprime random primer labeling kits (Invitrogen), immunoenriched DNA was labeled with Cy5 fluorophore, whole cell extract DNA was labeled with Cy3 fluorophore. Labeled DNA was mixed and hybridized to Agilent Human Promoter ChIP-on-chip Microarray Set for 20 hours at 40°C. The microarrays (Design ID - 014706 and 014707) have probes for about 17,000 human promoters. Arrays were then washed using standard Agilent protocols and scanned using an Agilent DNA microarray scanner BA. Scans were manually examined for abnormal features and intensities were extracted for each spot automatically using Agilent feature extraction software. We calculated the log of the ratio of median normalized intensity in the IP-enriched channel to median

normalized intensity in the genomic DNA channel for each probe and used a whole chip error model [64] to calculate confidence values for each spot on each array (single probe p-value). This error model functions by converting the intensity information in both channels to an X score which is dependent on both the absolute value of intensities and background noise in each channel. The X scores for an array are assumed to be normally distributed which allows for calculation of a p-value for the enrichment ratio seen at each feature. To determine bound regions in the datasets, we calculated the average X score of the 60-mer and its two immediate neighbors. If a feature was flagged as abnormal during scanning, we assumed it gave a neutral contribution to the average X score. Similarly, if an adjacent feature was beyond a reasonable distance from the probe (based on the maximum size of labeled DNA fragments hybridized to the array), we assumed it gave a neutral contribution to the average X score. This set of averaged values gave us a new distribution that was subsequently used to calculate p-values of average X (probe set p-values). If the probe set p-value was less than 0.001, the three probes were marked as potentially bound. In addition, the three probes in a probe set must each have single probe p-values < 0.05 or the center probe in the probe set has a single probe p-value < 0.01 and one of the flanking probes has a single point p-value < 0.1. Association with promoters was identified if the bound regions were 8kb upstream or 2 kb downstream of the Transcription Start Site[20]. Control experiments in cells expressing the negative control Tat_{SF2}G48-R57A showed only 34 positive signals, which is an acceptable background for ChIP-Chip experiments, supporting the specificity of the results observed with Ad-Tat_{SF2}. For conventional ChIP analysis the purified DNA was quantified by qPCR. The primers used in qPCR are described in Supplemental Table 2. Primers were designed near the site represented by the oligonucleotides present in the promoter arrays that provided a positive signal and were used for qPCR amplification of the corresponding sequences present in the immunoprecipitation-captured chromatin. 10 ng of immunoprecipitated DNA material and 10-90 ng of input (total) DNA samples were used in qPCR reactions. PCR products obtained by standard PCR for qualitative analysis were visualized on agarose gel with ethidium bromide.

Ingenuity Pathway analysis: The analysis for the identification of significant biological pathways and networks with whom ChIP-on-Chip derived genes are associated was carried out using Ingenuity Pathways Analysis software v7.6 (Ingenuity Systems, www.ingenuity.com). The canonical pathway analysis selects genes that have been previuosly identified as part of specific pathways and have been included the Ingenuity's Pathways Analysis library of canonical pathways. The p-value was calculated using the right-tailed Fisher Exact Test to determine the probability that the association between the genes in a dataset and the canonical pathway is explained by chance alone. With this method, the p-value for a given process annotation is calculated by considering (1) the number of focus genes that participate in that process and (2) the total number of genes that are known to be associated with that process in the selected reference set. Networks of genes were algorithmically generated based on their connectivity by overlaying the target genes onto a global molecular network developed from information contained in the Ingenuity Pathways Knowledge Base.

Kinase inhibitors and their specificity: AS601245 is potent JNK1/2 and JNK3 inhibitor and exhibits specific selectivity for JNK as compared to ERK1 and p38 *(Ferrandi C et al. (2004) Br J Pharmacol. 142(6): 953–960).*

SB203580 is a highly specific, ATP competitive inhibitor of p38 MAP kinase (IC50 = 34 nM *in vitro*, 600 nM in cells). It does not significantly inhibit the JNK and p42 MAP kinase (ERK) at 100 μM (*Rouse, J. et al. (1994) Cell 78, 1027-1037; Han, J. et al. (1994) Science 265, 808-811*). In our study we used it at 10 μM.

PD98059 (MEK1 Inhibitor) inhibits activation of MEK1 and MEK2 with IC50 values of 4 μM and 50 μM, respectively. It has been shown that PD98059 does not inhibit activation of other highly related dual-specificity protein kinases or the activity of over 18 other Ser/Thr protein kinases (*Rosen, L.B. et al. (1994) Neuron 12, 1207–1221*). At concentrations up to 100 μM, PD98059 does not inhibit activation of MKK3/6 or MKK4 as determined by measuring phosphorylation at its activation site.

Supplementary Table S1. Phenotypic marker expression on the KG-1 cells

Cell marker	Percentage of positive cells				
	untreated	GM-CSF/IL4	GM-CSF/IL4/TNF	PMA/TNF	human iDC
CD80	2	1.7	2	6.8	2.9
CD86	2	16	17.2	9.5	50
CD83	4	8.4	13	20.3	22
HLA-DR	23	29	31	36	50
CD14	-	-	-	-	-
CD1a	2.5	2	2.3	3.6	45
CD11c	19.5	34	61.2	39	82

KG-1 cells were cultured in medium alone, GM-CSF (100 ng/ml) and IL4 (50 ng/ml) with or without TNF-α (2.5 ng/ml), or PMA (10 ng/ml) plus TNF-α (10 ng/ml). The time of maximal expression varied depending on the stimulus. The data reported were observed after 5 days in culture.

Supplemental Table S2: Oligonucleotide sequences usedin RT-qPCR.

Gene	RefSeq no.	Primers	5' Oligo	3' Oligo	Size
IRF7	NM_001572	E1(+196/+325) E2(+1742/+1841)	CTGGACACTGGTTCAACACCT CCCCATCTTCGACTTCAGAG	GTGTGGACTGAGGGCTTGTAG CGAAGCCCAGGTAGATGGTA	130 100
IP10	NM_001565	E1(+238/+382)	CCACGTGTTGAGATCATTGC	ATTTTGCTCCCCTCTGGTTT	145
MAP2K3	NM_002756	E1(+39/+185) E2(+458/+587)	CCAGTCCAAAGGAAAATCCA CGGAAGGTGCTGGATAAAAA	TCAGCCTCCACCTCAAAGTT ACATTGGAGGGCTTCACATC	147 134
MAP2K4	NM_003010	E1(+270/+388) E2(+1051/+1188)	CCCTGAACAACACTGGGATT GATGAATCCAAAAGGCCAAA	CTGCCATTATTTGCCCACTT CATGGGAGAGCTGGGAGTAG	119 138
MAP2K6	NM_002758	E1(+252/+360) E2(+560/+694)	CCGAGCCACAGTAAATAGCC TCAATGCTCTCGGTCAAGTG	AAACAGTGCGCCATAAAAGG TCTGGTTGAGCTCTGGGTTT	109 135
MCP2	NM_005623	E1(+424/+559)	ACCTTCACCTCTCATGCTGAA	TGGAATGGAAACTGAATCTGG	136
MIG	NM_002416	E1(+2066/+2178)	GAAGCAGCCAAGTCGGTTAG	AATTCTGGCCACAGACAACC	123
STAT1	NM_007315	E1(+823/+923) E2(+1287/+1373)	TGAAATCAAGAGCCTGGAAGA TTCAGAGCTCGTTTGTGGTG	GATCACTCTTTGCCACACCAT TGAACTGGACCCCTGTCTTC	101 87
TRAIL	NM_003810	E1(+480/+620) E2(+1450/+1569)	ACCAGAGGAAGAAGCAACACA GGAACCCAAGGTGGGTAGAT	GACCAGTTCACCATTCCTCAA CTACAGGCATGTGCCAACAC	141 120

Oligonucleotide sequences used for ChIP-qPCR

Gene	Ref Seq no.	Primers	5' Oligo	3' Oligo
MAP2K3	NM_002756	P1(-474/-353) P2(-237/-108) P3(+12/+102)	TAGGGAGCTTGCTAGGGTGA CTGGCGGACTTGACAGAGA GCCTGAGTCAGCGCAGTT	ACCCGAGATCCCTAAAGGTG TTGGTCCTTTCGTTTCCAAG GACTGCAGCAAGGACGAGT
MAP2K4	NM_003010	P1(-629/-780) P2(-388/-194) P3(+109/+174)	AGCAGCAGGAGGAGAAAGAA CTGTGCAAAGCAATGGAAGA GAGAGGCCGAGCTTGCTG	TACCTGCACGTCTTCATTGC TCCCAGCCTCCTGAAATATG GCCATTGTTGGGAGTGAAGA
MAP2K6	NM_002758	P1(-1028/-894) P2(-398/-228) P3(-162/-17)	CGACCACGTTTCCTTAAATCA GCCAACCCAATCATCCATAC GGACGTCTGCGCACTAAGAT	GGCAGCTAAAAGCTCCAAACT ACGGGGTGTCAACATTTAGC AATGCACACCTTGCAAAACA
IRF7	NM_001572	P1(-443/-346) P2(-271/-139) P3(+74/+181)	ACACCAGCCTGACCAACATAG CCTGGGTAACAAAAGCGAAA GCTCTGGCACCCAGGTACT	CTCCCGAGTAGCTGGGATTAC AGGGGACAGAGCAAGACTCA CCCCAGCTCTTGGCTCTAC

Supplemental Table S3: Comparative analysis of Tat association with promoters in APC

Promoter analysis associated with HIV Tat in KG-iDC

Ingenuity Canonical Pathways	p-value	Molecules
IL-1 Signaling	1.86E-04	MAP2K4,PRKACB,MAP2K6, IL1A
p38 MAPK Signaling	3.62E-03	MAP2K4,MAP2K6,IL1A,TGFB3
cAMP-mediated signaling	4.80E-03	PRKACB,PKIA,AKAP7,RAP1A
Dendritic Cell Maturation	8.40E-03	MAP2K4,IL1A,PIK3R1
Toll-like Receptor Signaling	1.01E-02	MAP2K4,MAP2K6
RANK Signaling in Osteoclasts	1.03E-02	MAP2K4,MAP2K6,MAP3K9,MITF,PIK3R1
Inositol Phosphate Metabolism	1.06E-02	MAP2K4,MAP2K6,MAP3K9,SGK1,PIK3R1,PLCL2
HGF Signaling	1.06E-02	MAP2K4,MAP3K9,PIK3R1,RAP1A,ELF1
Neuropathic Pain Signaling In Dorsal Horn Neurons	1.22E-02	PRKACB,GRIN2A,PIK3R1,PLCL2,GRIA4
CD40 Signaling	1.28E-02	MAP2K4,MAP2K6,PIK3R1,TNFAIP3
Melatonin Signaling	1.31E-02	MAP2K4,PRKACB,MAP2K6,PLCL2
Insulin Receptor Signaling	1.51E-02	PRKACB,FYN,SGK1,PIK3R1,FOXO3,PPP1R11
Acute Myeloid Leukemia Signaling	1.57E-02	MAP2K4,MAP2K6,PIK3R1,CEBPA
Reelin Signaling in Neurons	1.67E-02	MAP2K4,FYN,MAP3K9,PIK3R1
CD27 Signaling in Lymphocytes	1.69E-02	MAP2K4,MAP2K6,MAP3K9
Integrin Signaling	1.70E-02	MAP2K4,ITGAD,FYN,PIK3R1,ITGA8,RAP1A
Synaptic Long Term Potentiation	1.76E-02	PRKACB,GRIN2A,PPP1R11,GRIA4,RAP1A
Amyotrophic Lateral Sclerosis Signaling	1.90E-02	GRIN2A,RAB5A,PIK3R1,GRIA4
HIF1α Signaling	1.95E-02	MMP7,MMP16,PIK3R1,SLC2A2
Nicotinate and Nicotinamide Metabolism	2.10E-02	MAP2K4,MAP2K6,MAP3K9,SGK1

Promoter analysis associated with HIV Tat in THP-Mac

Ingenuity Canonical Pathways	p-value	Molecules
p38 MAPK Signaling	1.78E-02	MAP2K4,MAP2K6,IL1A,TGFB3
IL-10 Signaling	6.22E-02	MAP2K6,IL1RAPL1
IL-1 Signaling	1.67E-02	MAP2K6,H3f3a/H3f3b,IL1RAPL1
Nicotinate and Nicotinamide Metabolism	1.10E-01	MAP2K6,CDK8
Estrogen Receptor Signaling	1.31E-01	CDK8,H3f3a/H3f3b
Selenoamino Acid Metabolism	1.49E-01	MAT1A
IL-6 Signaling	1.53E-01	MAP2K6,IL1RAPL1
Notch Signaling	1.61E-01	PSEN1
Methionine Metabolism	1.61E-01	MAT1A
Cell Cycle Regulation by BTG Family Proteins	1.90E-01	PPP2R3A
Hepatic Cholestasis	1.93E-01	IL1RAPL1,SLCO1B3
Role of PKR in Interferon Induction and Antiviral Response	2.02E-01	MAP2K6
Inositol Phosphate Metabolism	2.05E-01	MAP2K6,CDK8
Role of Macrophages, Fibroblasts and Endothelial Cells in Rheumatoid Arthritis	2.16E-01	MAP2K6,DAAM1,IL1RAPL1
PPARα/RXRα Activation	2.31E-01	MAP2K6,IL1RAPL1

Pathways listed in this table are linked to the pathways listed in Supplemental Table 4 directly or indirectly by virtue of gene expression regulation.

Supplemental Table S4: Comparative analysis of Tat gene expression in APC

Gene expression analysis modulated by HIV Tat in iDC

Ingenuity Canonical Pathways	p-value	Molecules
Interferon Signaling	7.59E-09	IFIT3,OAS1,IFITM1,MX1,IFI35,STAT1
Pathogenesis of Multiple Sclerosis	4.44E-08	CXCL10,CXCL9,CCL5,CCL3
Role of Pattern Recognition Receptors in Recognition of Bacteria and Viruses	1.24E-06	OAS1,IRF7,OAS2,CCL5,OAS3,TNF
Activation of IRF by Cytosolic Pattern Recognition Receptors	9.36E-09	IRF7,STAT1,IFIT2,TNF,ISG15
Role of Hypercytokinemia/hyperchemokinemia in the Pathogenesis of Influenza	4.66E-05	CXCL10,CCL5,CCL3,TNF
Differential Regulation of Cytokine Production in Macrophages and T Helper Cells by IL-17A and IL-17F	6.55E-05	CCL5,CCL3,TNF
Differential Regulation of Cytokine Production in Intestinal Epithelial Cells by IL-17A and IL-17F	1.22E-04	CCL5,CCL3,TNF
IL-17A Signaling in Gastric Cells	1.81E-04	CXCL10,CCL5,TNF
Hepatic Fibrosis / Hepatic Stellate Cell Activation	3.94E-04	CXCL9,CSF1,CCL5,STAT1,TNF
Communication between Innate and Adaptive Immune Cells	7.16E-04	CXCL10,CCL5,CCL3,TNF
TREM1 Signaling	1.78E-03	CCL7,CCL3,TNF
Role of MAPK Signaling in the Pathogenesis of Influenza	3.88E-03	CXCL10,CCL5,TNF
Glucocorticoid Receptor Signaling	6.18E-03	HSPA6,CCL5,STAT1,CCL3,TNF
TNFR2 Signaling	6.84E-03	TNFAIP3,TNF
IL-9 Signaling	1.06E-02	STAT1,TNF
Atherosclerosis Signaling	1.20E-02	CSF1,F3,TNF
Renin-Angiotensin Signaling	1.36E-02	CCL5,STAT1,TNF
Role of PKR in Interferon Induction and Antiviral Response	1.56E-02	STAT1,TNF
Role of IL-17F in Allergic Inflammatory Airway Diseases	1.06E-02	CXCL10,CCL7

Gene expression analysis modulated by HIV Tat in MDM

Ingenuity Canonical Pathways	p-value	Molecules
Interferon Signaling	9.94E-10	IFIT3,OAS1,IFNGR2,IFITM1,MX1,IFI35,STAT1
Pathogenesis of Multiple Sclerosis	1.45E-07	CXCL10,CXCL9,CCL5,CCL3
Role of Pattern Recognition Receptors in Recognition of Bacteria and Viruses	3.95E-07	OAS1,IRF7,OAS2,CASP1,C1QB,CCL5,OAS3
Activation of IRF by Cytosolic Pattern Recognition Receptors	3.87E-05	IRF7,NFKBIE,STAT1,IFIT2,ISG15
Thyroid Cancer Signaling	1.33E-04	CXCL10,TCF4,CCND1,TCF7L2
Hepatic Fibrosis / Hepatic Stellate Cell Activation	1.87E-04	CXCL9,FLT1,ACTA2,IFNGR2,CCL5,STAT1
Antigen Presentation Pathway	1.72E-03	PSMB9,HLA-DRB4,TAP2
Communication between Innate and Adaptive Immune Cells	2.12E-03	CXCL10,HLA-DRB4,CCL5,CCL3
Role of Hypercytokinemia/hyperchemokinemia in the Pathogenesis of Influenza	2.41E-03	CXCL10,CCL5,CCL3
TREM1 Signaling	4.06E-03	CCL7,CASP1,CCL3
Role of IL-17A in Arthritis	5.04E-03	CCL7,NFKBIE,CCL5
Differential Regulation of Cytokine Production in Macrophages and T Helper Cells by IL-17A and IL-17F	7.49E-03	CCL5,CCL3
Polyamine Regulation in Colon Cancer	7.49E-03	TCF4,OAZ1
Differential Regulation of Cytokine Production in Intestinal Epithelial Cells by IL-17A and IL-17F	8.88E-03	CCL5,CCL3
Role of JAK1, JAK2 and TYK2 in Interferon Signaling	9.61E-03	IFNGR2,STAT1
IL-17A Signaling in Gastric Cells	1.09E-02	CXCL10,CCL5

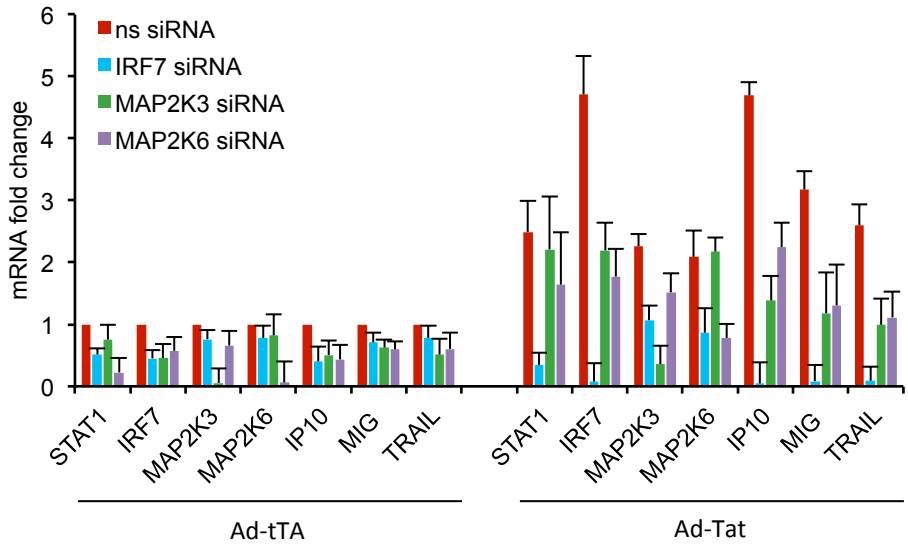

Figure S1. mRNA levels of cellular genes in THP-1 cells transfected for 48 hours with MAP2K6, MAP2K3, and IRF7 siRNA, infected for 24 hours with an Ad- $Tat_{SF2/}$Ad-tTA or Ad-tTA alone, and analyzed by RT-qPCR. Results are normalized to actin and reported as fold induction relative to Ad-tTA infected cells treated with ns siRNA. The average of three independent experiments is shown.